Nelfinavir Down-regulates Hypoxia-Inducible Factor 1α and VEGF Expression and Increases Tumor Oxygenation: Implications for Radiotherapy

Nabendu Pore,[1] Anjali K. Gupta,[1] George J. Cerniglia,[1] Zibin Jiang,[1] Eric J. Bernhard,[2] Sydney M. Evans,[1] Cameron J. Koch,[1] Stephen M. Hahn,[1] and Amit Maity[1]

[1]Department of Radiation Oncology, University of Pennsylvania School of Medicine, Philadelphia, Pennsylvania and [2]Departments of Radiation Oncology and Biology, Oxford University, 4A122 John Radcliffe Hospital, Headington Oxford, United Kingdom

Abstract

The phosphatidylinositol 3-kinase (PI3K)/Akt pathway can increase vascular endothelial growth factor (VEGF) and hypoxia-inducible factor 1α (HIF-1α) expression. We examined the effect of nelfinavir, an HIV protease inhibitor that inhibits Akt signaling, on VEGF and HIF-1α expression and on angiogenesis, tumor oxygenation, and radiosensitization. Nelfinavir decreases VEGF expression under normoxia via the transcription factor Sp1, which regulates the proximal core VEGF promoter. Nelfinavir decreased Sp1 phosphorylation and decreased Sp1 binding to a probe corresponding to the proximal VEGF promoter in a gel shift assay. Nelfinavir also decreased the hypoxic induction of HIF-1α, which also regulates the VEGF promoter, most likely by decreasing its translation. The effect of nelfinavir on VEGF expression had the functional consequence of decreasing angiogenesis in an *in vivo* Matrigel plug assay. To determine the effect this might have on tumor radiosensitization, we did tumor regrowth assays with xenografts in nude mice. The combination of nelfinavir and radiation increased time to regrowth compared with radiation alone whereas nelfinavir alone had little effect on tumor regrowth. This radiosensitizing effect was greater than suggested by *in vitro* clonogenic survival assays. One possible explanation for the discordance is that nelfinavir has an effect on tumor oxygenation. Therefore, we examined this with the hypoxia marker EF5 and found that nelfinavir leads to increased oxygenation within tumor xenografts. Our results suggest that nelfinavir decreases HIF-1α/VEGF expression and tumor hypoxia, which could play a role in its *in vivo* radiosensitizing effect. These data support the use of nelfinavir in combination with radiation in future clinical trials. (Cancer Res 2006; 66(18): 9252-9)

Introduction

Recently, it was shown that protease inhibitors such as nelfinavir, currently used to treat HIV patients, can radiosensitize tumor cells, possibly via inhibition of phosphatidylinositol 3-kinase (PI3K)/Akt signaling (1). The PI3K/Akt pathway is commonly activated in many cancers through diverse mechanisms including loss of the tumor suppressor phosphatase and tensin homologue, amplification of PI3K subunits, overexpression of Akt, and mutations in the PI3K subunits (2–4). This pathway has been implicated in many cellular processes including cell proliferation, adhesion, migration, invasion, and apoptosis (4–7). The PI3K/Akt pathway can also regulate hypoxia-inducible factor 1α (HIF-1α) expression (8, 9). HIF-1α is one subunit of a heterodimeric transcription factor that binds to a specific consensus sequence (5′-RCGTC-3′). The other subunit, HIF-1β, remains fairly constant in level during hypoxia and normoxia. In contrast, the level of HIF-1α is very low in normoxia in most cell lines but is induced by hypoxia. When both components are present, the heterodimer binds to the consensus sequence found in dozens of hypoxia-inducible genes that control a wide range of processes including angiogenesis (*VEGF*), glycolysis, glucose uptake (*glut1*), and tumor invasion and metastasis (reviewed in ref. 10).

The PI3K/Akt pathway can also regulate the expression of vascular endothelial growth factor (VEGF; ref. 11). VEGF is often overexpressed in cancers and may be critical for growth beyond a certain size. This is underscored by the fact that therapeutic strategies to inhibit VEGF expression and function, including antibodies, kinase inhibitors, and soluble VEGF receptors, efficiently inhibit tumor growth in animal models (12).

Because the drug nelfinavir can inhibit PI3K/Akt signaling, we examined the effect of this drug on the expression of both VEGF and HIF-1α. We found that nelfinavir deceased the expression of both proteins and was associated with a modest degree of radiosensitization *in vitro*. The radiosensitizing effect of nelfinavir *in vivo* was much larger than expected. The origin for this therapeutically advantageous result seems to be related to reoxygenation.

Materials and Methods

Tissue culture and reagents. SQ20B head and neck squamous cell carcinoma and A549 lung carcinoma cells were cultured in DMEM (4,500 mg/L glucose; Invitrogen, Carlsbad, CA) containing 10% fetal bovine serum (Atlanta Biologicals, Lawrenceville, GA) and grown in an incubator containing 5% CO_2 and 21% O_2. Hypoxic conditions were established as previously described (13).

Northern blot analysis. Total RNA was isolated with RNazol (Life Technologies) following the directions of the manufacturer. Ten to fifteen micrograms of RNA were denatured with formaldehyde and formamide and run on a 0.9% agarose gel containing formaldehyde. RNA was transferred by capillary action in 20× SSC [1× SSC is 0.15 mol/L NaCl, 0.15 mol/L sodium citrate (pH 7)] to a Duralon-UV membrane (Stratagene, La Jolla, CA) and UV cross-linked before hybridization. Labeling of radioactive probes was done with [^{32}P]dCTP and a Prime-It kit (Stratagene) according to the directions of the manufacturer. Hybridization was carried out at 65°C, after which the membranes were washed with 0.1 × SSC, 0.1% SDS at 65°C. Autoradiography was carried out at −80°C with intensifying screens.

Note: Supplementary data for this article are available at Cancer Research Online (http://cancerres.aacrjournals.org/).

Requests for reprints: Amit Maity, University of Pennsylvania School of Medicine, 195 John Morgan Building, 3620 Hamilton Walk, Philadelphia, PA 19104. Phone: 215-614-0078; Fax: 215-898-0090; E-mail: maity@xrt.upenn.edu.

doi:10.1158/0008-5472.CAN-06-1239

A 200-bp VEGF cDNA fragment excised with *Eco*RI from the pGEMh204 plasmid was used to make radioactive probes for hybridization. A fragment for HIF-1α Northern blotting was excised from a plasmid containing the HIF-1α cDNA (gift from G. Semenza, Johns Hopkins University School of Medicine, Baltimore, MD). To verify equal loading between lanes, all gels were stained with ethidium bromide and the membranes were probed with a DNA fragment of the 18S rRNA.

Protein extraction and Western blot analysis. For protein isolation, cells were washed once with cold PBS containing 1 mmol/L EDTA, then solubilized by adding lysis buffer [1% Triton X-100, 20 mmol/L Tris (pH 7.6), 150 mmol/L NaCl, 2 mmol/L EDTA, 10% glycerol, 1 mmol/L DTT, 1 mmol/L orthovanadate, 2 mmol/L phenylmethylsulfonyl fluoride] directly on the cells. Lysates were transferred into 1.5-mL Eppendorf tubes and centrifuged at 12,000 rpm for 10 minutes at 4°C. Supernatants were transferred to a fresh tube and frozen on dry ice. Protein concentrations were determined with a bicinchoninic acid (BCA) Protein Assay kit (Pierce, Rockford, IL). For Western blotting, an equal amount of total protein was separated by SDS/PAGE on a 6% polyacrylamide gel. For Western blotting, equal amounts of total protein were run in each lane of an SDS-PAGE gel (12% acrylamide). Each protein sample was mixed with an equal volume of 2× Laemmli buffer and boiled at 95°C for 5 minutes before loading onto the gel. After completion of gel electrophoresis, protein was transferred to a Hybond nitrocellulose membrane (Amersham-Pharmacia, Piscataway, NJ) over 1 hour using a blotting apparatus. The following antibodies were used: monoclonal anti–phospho-Akt antibody that recognizes phospho-Akt (Ser^{473}) (New England Biolabs, Ipswich, MA), anti-Akt antibody, anti-HIFα antibody (clone H1α67, Novus Biologicals, Littleton, CO) at 1:1,000 dilution, and anti-β-actin antibody (Sigma-Aldrich, St. Louis, MO) at 1:1,000 dilution. The secondary antibody used for these blots was a goat anti-mouse antibody (Bio-Rad, Hercules, CA). Antibody binding was detected by chemiluminescence using an enhanced chemiluminescence kit (Amersham Pharmacia, Piscataway, NJ).

Plasmid constructs and transient transfections. Construction of the plasmids pGL3-1.5 kbVEGFprom and mut1 has been previously described (13). Transfections were done with FuGENE (Roche, Nutley, NJ) according to the instructions of the manufacturer. Briefly, cells were split into 60-mm dishes so that, 24 hours later, they were ~50% confluent. At this time, each dish was transfected with 6 μL of FuGENE and 2 μg of the reporter plasmid and, to control for transfection efficiency, 1 μg of pSV-β-galactosidase (Promega, Madison, WI). Cells were harvested by removing the medium, washing twice with PBS, and directly adding 100 μL of lysis buffer per dish. Of this lysate, 80 μL were used for luciferase determinations and 10 μL for β-galactosidase assays. These determinations were done with the LucLite kit (Perkin-Elmer, Wellesley, MA) and the β-Galactosidase Enzyme Assay System (Promega). Luciferase readings were done on a TopCount Microplate Scintillation and Luminescence Counter (Packard Instrument).

Adenovirus. Adenovirus expressing myristoylated Akt, capable of replicating in the "packaging" 293 cell line, was made using the pAd-Easy protocol as previously described (13). The virus was stored in single-use aliquots at −80°C. Cells were infected at multiplicities of infection of 5 to 10 and cells were harvested 48 hours postinfection.

Gel shift assay. Nuclear proteins were extracted as previously described (14). Oligonucleotides corresponding to −88 to −66 bp of the human VEGF/VPF promoter were synthesized. The complementary sequences 5′-CCGGGGCGGGCCGGGGGCGGGGGT-3′ and 5′ ACCCCGCCCCCGGCCC-GCCCCGG-3′ were labeled with [γ-^{32}P]ATP and T4 polynucleotide kinase. Unincorporated [γ-^{32}P]ATP were removed by centrifugation through G-25 Sephadex column (Boehringer Mannheim) according to the recommendations of the manufacturer. The DNA-binding reaction was done for 30 minutes at room temperature in a volume of 20 μL containing 5 μg of nuclear protein extract, 2.5 mg/mL bovine serum albumin, 10^5 cpm, 0.1 mg/mL poly[dI:dC] (Sigma), and 5 μL of 4× binding buffer [1× buffer: 10 mmol/L Tris-Cl (pH 7.8), 100 mmol/L KCl, 5 mmol/L $MgCl_2$, 1 mmol/L EDTA, 10% (v/v) glycerol, 1 mmol/L DTT] with or without excess of unlabeled competitor or Sp1 consensus-oligonucleotide (Promega). Samples were subjected to electrophoresis on a native 5% polyacrylamide gel run in 0.5× TGE (50 mmol/L Tris-HCl, 400 mmol/L glycine, 2 mmol/L EDTA) for 2.5 hours at 120 V.

Orthophosphate labeling and Sp1 immunoprecipitation. Cells were incubated in phosphate-free DMEM (Life Technologies) for 1 hour, labeled in medium containing 1 mCi [^{32}P]orthophosphate (Amersham Pharmacia) for 8 hours, and harvested with sample lysis buffer as described above for Western blotting.

The protein solution was precleared with agarose A (Invitrogen, Carlsbad, CA) and incubated with an anti-Sp1 antibody (Sigma-Aldrich) at 4°C overnight. Immunoprecipitates were isolated with protein A and the beads were washed four times with buffer. Finally, beads were resuspended in 50 μL of 1× SDS-PAGE loading buffer [0.06 mol/L Tris-HCl (pH 8.0), 1.71% SDS, 6% glycerol, 0.1 ml/L 0.002% bromophenol blue] and boiled at 95°C. The released proteins were separated on 12% SDS-PAGE gel. Separated proteins were transferred to a Hybond nitrocellulose membrane (Amersham-Pharmacia) and autoradiographed.

[^{35}S]Met-Cys labeling and HIF-1α immunoprecipitation. Medium was replaced with Met-Cys–free DMEM containing 5% serum. After 30 minutes, [^{35}S]Met-Cys was added to a final concentration of 0.2 mCi/mL, and the cells were pulse labeled for 2 hours in the presence of DMOG and then harvested. Cells were washed once in ice-cold PBS, trypsinized, then centrifuged. The ellets were then solubilized in sample lysis buffer described above for Western blotting. The protein solution was passed repeatedly through a 26-gauge needle. Thereafter, samples were centrifuged at 10,000 × *g* and the supernatants were retained. Fifty microliters of Protein A-Sepharose beads were added to the cell lysate in an Eppendorf tube and incubated on ice for 30 to 60 minutes. Then the mixture was centrifuged at 10,000 × *g* for 10 minutes at 4°C. The supernatant was transferred to a fresh Eppendorf tube and proteins were quantified with the BCA kit (Pierce). Equal amount of total protein (1 mg) was taken in an Eppendorf tube and 10 μg of anti-HIF-1α antibody (H1α67; Novus Biologicals) were added and then incubated at 4°C for 16 hours. Then, 50 μL of washed Protein G slurry in prechilled sample lysis buffer were added and incubated for 1 hour at 4°C. Thereafter, the immunoprecipitated proteins were centrifuged at 10,000 × *g* for 30 seconds at 4°C thrice. The supernatant was removed completely and the beads were washed thrice with 500 μL of lysis buffer. After the last wash, supernatant was aspirated and 50 μL of 1× Laemmli sample buffer were added to the bead pellet and heated to 90°C to 100°C for 5 minutes. Then the Eppendorf tube was centrifuged at 10,000 × *g* for 5 minutes and the supernatant was loaded onto a gel.

***In vitro* radiation survival studies.** Cells in exponential growth phase were counted and plated in 60-mm dishes containing 4 mL of medium. The cells were allowed to attach for 4 hours, then nelfinavir was added to cultures 1 hour before radiation. Cells were irradiated with a Mark I cesium irradiator (J.L. Shepherd, San Fernando, CA) at a dose rate of 1.6 Gy/min. Colonies containing >50 cells were stained and counted 10 to 14 days after irradiation. The surviving fraction was calculated by dividing the number of colonies formed by the total number of cells plated, times plating efficiency. Each point on the survival curve represents the mean surviving fraction from at least three replicates.

Tumor xenografts generation and nelfinavir treatment. Pathogen-free female Ncr-*nu/nu* mice were obtained from Taconic Industries (Germantown, NY) and housed in the animal facilities of University Laboratory Animal Resources and the Institute for Human Gene Therapy of the University of Pennsylvania. All experiments were carried out in accordance with University Institutional Animal Care and Use Committee guidelines. When the mice were 5 to 7 weeks of age, tumors were initiated in the flank by s.c. injection of 1×10^6 A549 cells suspended in 100 μL of Matrigel (BD Collaborative Research, Franklin Lakes, NJ). Tumors were palpable between 5 and 7 days postinoculation.

Before the start of experiments, feed consumption was measured for each mouse daily for 5 days. The average feed consumed per day was used to define the amount of feed each mouse was given daily during the 5-day course of nelfinavir treatment (4 g/d). The feed was a Transgenic dough diet (Bioserve, Frenchtown, NJ) and contained 1.58 mg of nelfinavir. Based on an average weight of 20 g for a mouse, this delivered 79 mg nelfinavir/kg/d.

During the experiments, all the feed was eaten and no additional feed was given that day.

EF5 detection of hypoxia. EF5 is a 2-nitroimidazole that forms covalent protein adducts in viable hypoxic cells in a manner that is inversely proportional to oxygen concentration in the physiologic range (15–17). Details about its use in assessing tumor oxygenation in human tumors and human tumor xenografts in rodent models are provided elsewere (18, 19). Briefly, mice were injected with 10 mmol/L drug in 2.4% ethanol and 5% dextrose i.v. (0.01 ml/g body weight), followed by an equal volume i.p. injection 30 minutes later. Three hours after the first EF5 injection, mice were euthanized. The tumor was resected and frozen, then sections (10 μm) were cut onto poly-L-lysine–coated slides, fixed in 4% paraformaldehyde for 1 hour, and then rinsed and blocked for 2 hours at room temperature. Slides were stained with Cy3-conjugated ELK3-51, a mouse monoclonal antibody to EF5.

Photomicroscopy image analysis. Epifluorescence measurements were made with a Nikon LabPhot microscope (Nikon, Melville, NY) with a 100-W high-pressure mercury arc lamp. Filter cubes were optimized for wavelengths of interest (Omega Optical, Brattleboro, VT). Data were captured with a cooled (225°C) charge-coupled device digital camera (Photometrics Quantix KF1400, Photometrics, Tucson, AZ). Each image field (at ×10 magnification) consisted of 600 × 400 pixels corresponding to 1.05 × 0.7 mm^2. Images were all grayscale TIFF images; raw 12-bit data from the camera were converted to 8 bit (value from 0 to 255) before analysis containing intensity values from 0 to 255. Images were analyzed with Adobe Photoshop software (Adobe Systems, Inc., San Jose, CA). Variations in the lamp intensity were accounted for by measuring the fluorescence of a reference concentration of Cy3. This reference intensity was used in each instance to normalize the intensities of images captured from tumor sections at the time of analysis.

Analysis of *in situ* EF5 binding. For the purpose of image analysis, bitmap (two-color) masks were created of the Hoechst 33342 images in Adobe PhotoShop by applying the auto level function to enhance contrast followed by maximum and median filters to spread the nuclear-localized fluorescence over the approximate diameter of a cell. Thresholding was done to create a mask of tissue-containing areas. EF5-dependent fluorescence intensity values were sampled within an image based on tissue location identified by the Hoechst 33342 mask.

Just before imaging, tissue sections were dipped briefly into a 25 μmol/L Hoechst 33342 solution. This stains the nuclei, which can then also be imaged, before the imaging of EF5 or CD31 over the same coordinates.

EF5 intensity values at the 95% binding level were determined from EF5 binding in all tumor tissue on a section, identified by the Hoechst mask. The 95% binding values were calibrated based on lamp intensity and exposure time. Final values for *in situ* EF5 binding were obtained by subtracting the value for nonspecific binding (competed stain) in an adjacent section from that of regular stain binding (20).

***In vivo* study of angiogenesis using Matrigel plug assay.** This assay was done as previously described (21). Angiogenesis was measured in growth factor–free Matrigel (Collaborative Biomedical Products, Inc., Bedford, MD). The Matrigel plug (500 μL) containing 2 × 10^6 cells of each cell line was injected s.c. into the right and left side of 4- to 8-week-old female BALB/c nude mice at sites lateral to the abdominal midline. As a negative control, Matrigel with 100 μL PBS was injected in similar manner. All measurements were made in triplicate. Animals were sacrificed 5 days after Matrigel injection. The Matrigel plugs were recovered and photographed immediately. Plugs were then dispersed in PBS and incubated at 4°C overnight. Hemoglobin levels were determined with Drabkin's solution (Sigma-Aldrich, St. Louis, MO) according to the instructions of the manufacturer.

Determination of tumor regrowth delay. Mice bearing A549 tumors were randomly assigned a treatment group (radiation plus drug, radiation alone, drug alone, or mock treatment). Mice were pretreated for 5 days with nelfinavir given orally as previously detailed. Irradiation (8 Gy) of the flank bearing the tumor was done with a 250-kV orthovoltage irradiator (Philips RT 250) at a dose rate of 2.63 Gy/min through a 0.2-mm copper filter. The source-to-tumor target distance was 30 cm with shielding of nontumor sites. Mice were examined twice weekly for evaluation of tumor growth. Tumors were measured with calipers in three mutually perpendicular diameters (*a, b*, and *c*) and the volume was calculated as $V = (\pi/6) \times a \times b \times c$.

Statistical analysis. As described in previous publications (1, 22), a regression model was fit to time to tumor volume of 1,000 mm^3 data that included terms to estimate the individual (main) effects of radiation and nelfinavir (NLF) and the interaction of these two treatments on the tumor regrowth. The linear model took the form

$$Y = \beta_0 + \beta_1(\text{radiation}) + \beta_2(\text{NLF}) + \beta_3(\text{radiation} \times \text{NLF})$$

where Y is the number of days to reach a volume of 1,000 mm^3 during the observation period; radiation and NLF are indicators for the treatment received (1 = yes, 0 = no); and radiation × NLF is an interaction term. The test of synergy between radiation and NLF was conducted on the interaction term using a one-sided Wald statistic to determine whether $\beta_3 > 0$, indicating synergy. $P = 0.05$ was considered to be significant. All analyses were done with SPSS 12.0 (SPSS, Inc., Chicago, IL).

Results

Involvement of Akt pathway in the down-regulation of VEGF expression. Nelfinavir lowered the level of Akt phosphorylation at Ser^{473} in both SQ20B head and neck squamous cell carcinoma cells and A549 lung carcinoma cells (Fig. 1*A*). Phospho-Akt levels were decreased by 24 hours and had almost completely disappeared by 72 hours whereas the total Akt and β-actin levels were unchanged. Nelfinavir treatment also decreased secreted VEGF protein in both SQ20B and A549 cells (Fig. 1*B*).

To investigate the role of the PI3K/Akt pathway in the regulation of VEGF expression by nelfinavir, we treated SQ20B cells with the PI3K inhibitor LY24002, nelfinavir, or both. Figure 1*C* shows that both nelfinavir and the PI3K inhibitor LY294002 led to an equivalent decrease in secreted VEGF in SQ20B cells. The combination of the two had no greater effect, consistent with the notion that the two agents act along the same pathway. Nelfinavir decreased the expression of VEGF mRNA expression in these cells, indicating that the effect of the drug was either transcriptional or at the level of RNA stability (Fig. 1*D*, compare *lanes 1* and *2*).

To assess where along the PI3K/Akt pathway nelfinavir might affect VEGF mRNA expression, we transduced SQ20B cells with either control or Akt-expressing adenovirus and treated them with either nelfinavir or control. Akt virus led to increased VEGF mRNA expression in SQ20B cells (Fig. 1*D*, compare *lanes 3* and *4*). However, nelfinavir treatment prevented Akt virus from substantially increasing the level of VEGF mRNA (Fig. 1*D*, compare *lanes 5* and *6*). This result suggests that nelfinavir acts either at the level or downstream of Akt in regulating VEGF expression.

Involvement of Sp1 in the down-regulation of VEGF by nelfinavir in normoxia. We have previously shown that Akt can regulate VEGF expression by transcriptionally regulating the proximal −88/+54 bp region of the VEGF promoter (13). To determine whether nelfinavir regulates VEGF at the transcriptional level, we did transient transfection experiments with luciferase reporters (shown in Supplementary Fig. S1). Exposure of cells transfected with the 1.5-kbp wild-type VEGF promoter to nelfinavir resulted in a decrease in reporter activity (Fig. 2*A*). The activity of a luciferase construct containing the −88/+54 region of the promoter was down-regulated to an even greater extent by nelfinavir. These observations suggest that elements within this region are responsive to the drug. Figure 2*A* also shows that mutation of

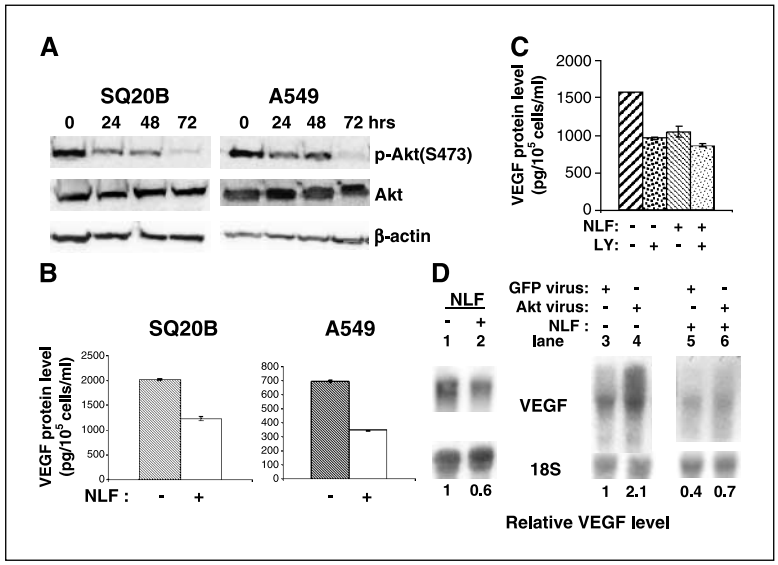

Figure 1. Nelfinavir decreases VEGF expression through PI3K/Akt pathways. *A,* A549 and SQ20B cells were treated with nelfinavir (*NLF*; 15 μmol/L) for various time points as indicated. Then cells were harvested and Western blotting was done. The membrane was probed for phospho-Akt (Ser^{473}) and total Akt and then was reprobed for β-actin (loading control). *B* and *C,* cell culture medium was sampled 30 hours after treatment of nelfinavir and/or LY294002 on A549 or SQ20B. VEGF protein levels were determined by ELISA and normalized to the number of cells present in each dish at the time the cell culture medium was sampled. *D, lanes 1* and *2,* SQ20B cells were treated with 15 μmol/L nelfinavir for 30 hours. *Lanes 3* to *6,* SQ20B cells were infected with adenovirus expressing activated Akt (myristoylated) or green fluorescent protein (*GFP*; control). After 24 hours of infection, cells were treated with nelfinavir or carrier for further 24 hours. Cells were harvested for RNA and Northern blotting was done for VEGF and subsequently for 18S (loading control). Relative RNA level indicates ratio of VEGF to 18S density.

the Sp1 binding sites within this −88/+54 bp region (Sp1mut construct in Supplementary Fig. S1) decreased the basal level of promoter activity and made it unresponsive to nelfinavir, suggesting that these sites were likely involved.

To further test the role of Sp1 in the response to nelfinavir, we did a gel shift assay, which showed that nelfinavir treatment dramatically decreased retardation of a labeled DNA oligonucleotide corresponding to the −88/−66 region of the promoter (Fig. 2*B*). Binding to this fragment could be effectively competed away by using excess cold Sp1 consensus probe. Phosphorylation of Sp1 has been implicated with increased binding of the transcription factor to consensus sites within various promoters (23–25). We also did *in vivo* orthophosphate labeling and showed that nelfinavir virtually eliminates Sp1 phosphorylation, which could explain how it leads to decreased Sp1 binding to the promoter (Fig. 2*C*).

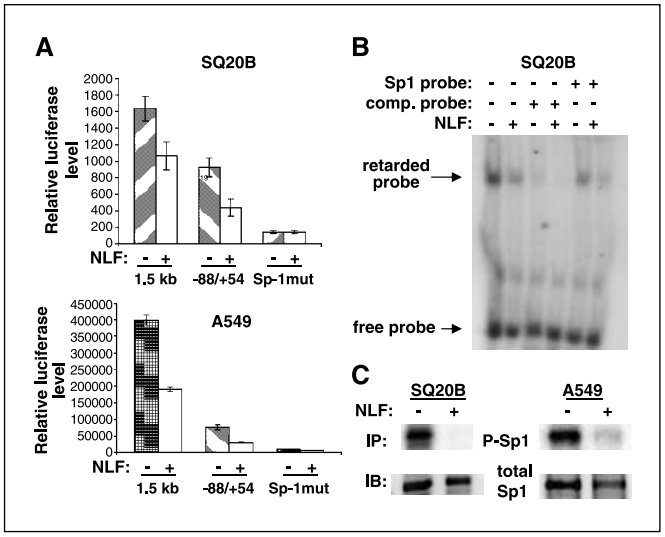

Figure 2. Nelfinavir decreases VEGF expression via activation of Sp1 transcription factors. *A,* SQ20B and A549 cells were transfected with 1.5 kb, −88/+54, and Sp1mut VEGF promoters. After 24 hours of transfection, cells were treated with nelfinavir (15 μmol/L) or control carrier. In each experiment, pSV-β-galactosidase was cotransfected along with the reporter constructs. *Y axis,* ratio of Luciferase and β-galactosidase activity. *B,* oligonucleotides corresponding to −88 to −66 bp of the human VEGF promoter were labeled with [γ-^{32}P]ATP. Gel shift assay was done using nuclear extract from SQ20B cells treated with nelfinavir or carrier (control). The DNA-binding reaction was done with 100-fold molar excess of unlabeled −88/−66 oligonucleotides (*comp. probe*) and/or Sp1 consensus oligonucleotides (*Sp1 probe*) as indicated. *C,* SQ20B and A549 cells treated with nelfinavir (15 μmol/L) were *in vivo* labeled with orthophosphate. Labeled proteins were immunoprecipitated with Sp1 antibody. Immunoprecipitated complexes were separated on gel and transferred to nitrocellulose membrane and autoradiographed. In the bottom part of gel (*IB,* immunoblot), the same membrane was probed with Sp1 antibody to serve as a loading control.

Nelfinavir down-regulates HIF-1α expression. Nelfinavir decreased the induction of HIF-1α in response to hypoxia (Fig. 3*A*), consistent with reports implicating the PI3K/Akt pathway in the regulation of HIF-1α (21). As expected, the drug also blunted the induction of VEGF mRNA, a well-known HIF-1 target, in response to hypoxia (Fig. 3*B*). Nelfinavir could decrease HIF-1α protein expression by (*i*) decreasing HIF-1α mRNA expression, (*ii*) decreasing HIF-1α protein translation independent of a change in the level of the mRNA, or (*iii*) decreasing HIF-1α protein stability. The first possibility was ruled out by showing that the level of HIF-1α mRNA did not change even after 48 hours of nelfinavir treatment (Fig. 3*C*). If nelfinavir decreased HIF-1α protein expression by decreasing its stability, treatment with proteasomal inhibitors, which stabilize HIF-1α, should prevent this decrease. However, we found that the proteasomal inhibitor MG132 allowed for accumulation of HIF-1α in control cells not treated with nelfinavir but failed to do so in nelfinavir-treated cells (Fig. 3*D*, compare *lanes 3* and *5* or *lanes 8* and *11*). This strongly suggested that nelfinavir does not act by destabilizing HIF-1α but rather by decreasing its synthesis. To directly investigate this possibility, we did metabolic labeling analysis. SQ20B cells were pulse labeled by [^{35}S]Met-Cys incorporation, followed by immunoprecipitation of HIF-1α. Under normoxia, little HIF-1α was recovered due to its rapid degradation (Fig. 3*E, lane 1*). However, in cells exposed to hypoxia, more HIF-1α was immunoprecipitated, but this was decreased by the pretreatment of cells with nelfinavir (Fig. 3*E*, compare *lanes 2* and *3*). Immunoblots using the lysates were probed for β-actin to show that the total amount of protein was the same in the different lanes. Therefore, Fig. 3*E* confirms that nelfinavir leads to decreased HIF-1α translation.

Nelfinavir down-regulates VEGF expression *in vivo*. To verify that nelfinavir had the same effect on VEGF expression *in vivo*,

SQ20B or A549 cells were implanted s.c. into nude mice. Mice were fed a diet containing nelfinavir or control carrier. After 4 days of nelfinavir treatment, mice were sacrificed and their tumors were removed. The tumors were lysed and Western blotting was done for VEGF. Figure 4*A* shows that nelfinavir treatment led to a decrease in VEGF expression in these tumor cells *in vivo*, consistent with our tissue culture results.

Nelfinavir decreases angiogenesis *in vivo*. To determine whether the decreased VEGF secretion seen in tumors grown in mice treated with nelfinavir had functional consequences, we did *in vivo* Matrigel assays. SQ20B or A549 cells were placed into Matrigel plugs, which were formed by s.c. injection into nude mice. Five days later, plugs were excised and evaluated for hemoglobin content. Nelfinavir significantly decreased angiogenesis visually and as determined quantitatively by hemoglobin measurement (Fig. 4*B* and *C*).

Radiation sensitization by nelfinavir. The data above clearly show that nelfinavir can down-regulate HIF-1α and VEGF expression. There are a number of studies that report that inhibition of VEGF and/or HIF-1α can increase radiosensitization (26–29). Therefore, we investigated the effect of nelfinavir on the response of A549 cells to radiation. Clonogenic cell survival experiments were done to determine any *in vitro* changes in radiosensitivity. Results from these experiments showed that A549 cells were sensitized to the cytotoxicity of ionizing radiation following exposure to nelfinavir (Fig. 5*A*).

In vivo radiation sensitization was assessed with the tumor regrowth delay assay. Mice bearing A549 tumors were randomly assigned to each treatment group (radiation plus drug, radiation alone, drug alone, or mock treatment). Mice were pretreated for 5 days with nelfinavir before irradiation (8 Gy). The results are shown in Fig. 5*B*. The mean time to tumor volume of 1,000 mm^3 was 17 days in the control group, the nelfinavir alone group, and the radiation alone group. The mean value increased to 27 days in the radiation and nelfinavir group. As seen in Fig. 5*C*, a statistically significant synergistic effect between radiation and nelfinavir was detected by proportional hazards regression analysis ($P = 0.01$).

Nelfinavir increases tumor oxygenation *in vivo*. The data in Fig. 5 suggest that the effect of nelfinavir on the radiation response is more dramatic *in vivo* than *in vitro*. Because pO_2 is recognized to be an important determinant of the radiation response, we wanted to examine the effect of nelfinavir on oxygenation. To do this, we did studies using the 2-nitroimidazole EF5, which binds to regions of hypoxia in a manner that is inversely proportional to oxygen concentration. EF5 was injected after 5 days of nelfinavir treatment. Mice were sacrificed 3 hours after EF5 injection. Images of tumors were acquired after immunohistochemical staining for EF5 (Fig. 6*A*) and the quantititative data are presented as the staining intensities of the brightest 5% of cells on an absolute fluorescence scale (Fig. 6*B*).

Discussion

The PI3K/Akt pathway has been implicated in the regulation of both HIF-1α and VEGF expression (8, 9, 30). We show in the present study that nelfinavir, a drug known to inhibit PI3K/Akt signaling (1), decreases both VEGF and HIF-1α expression. We previously showed that activation of the PI3K/Akt pathway leads to increased phosphorylation of the Sp1 transcription factor, which increases binding of the Sp1 transcription factor to sites

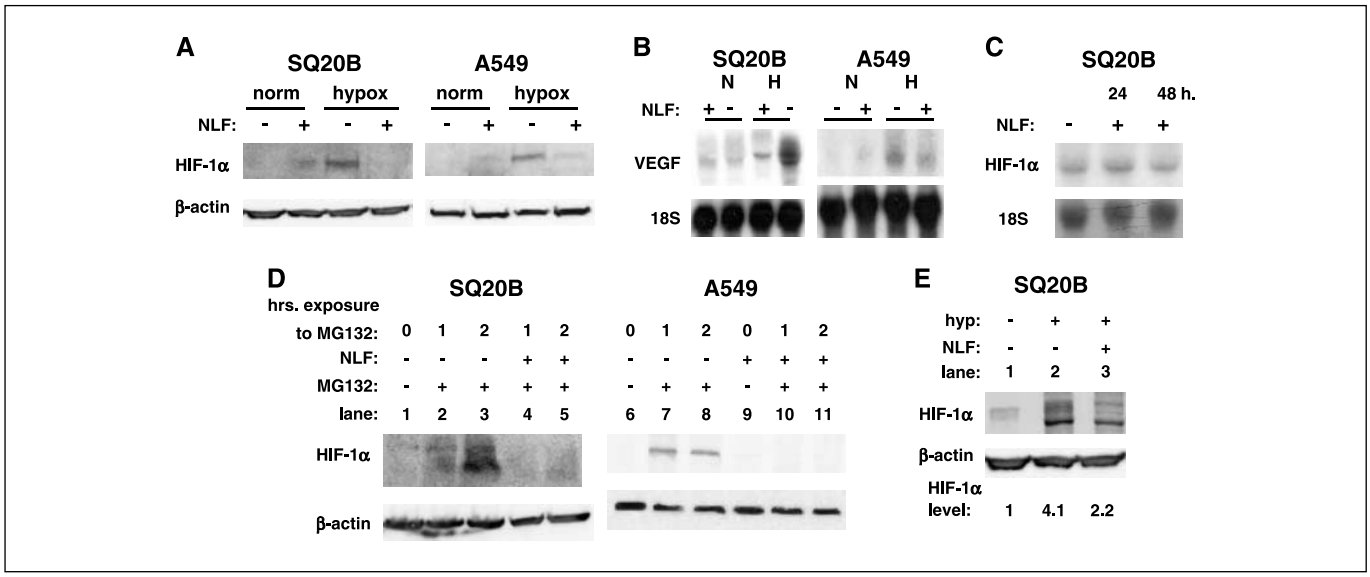

Figure 3. Nelfinavir decreases HIF-1 expression in A549 and SQ20B cells. *A,* A549 and SQ20B cells were treated with nelfinavir (15 μmol/L) for 30 hours and thereafter cells were exposed to hypoxia (0.2%) for 3 hours. Then cells were harvested and Western blotting was done with HIF-1α antibody. Subsequently, membranes were reprobed for β-actin. *B,* SQ20B and A549 cells were treated with 15 μmol/L nelfinavir for 24 hours; thereafter, cells were exposed to hypoxia (1%) for another 12 hours. Then cells were harvested for RNA and Northern blotting was done for VEGF and subsequently for 18S (loading control). *C,* SQ20B cells treated with nelfinavir (15 μmol/L) for indicated time period. Then cells were harvested for RNA and Northern blotting was done for HIF-1 message and subsequently for 18S (loading control). *D,* cells were pretreated with nelfinavir for 15 hours and then with the proteasomal inhibitor MG132 for different time periods (as indicated); thereafter, cells were harvested and Western blotting was done for HIF-1α. *E,* metabolic labeling experiments. SQ20B cells were treated with nelfinavir, and after 30 hours, regular medium was replaced with DMEM (Met-Cys–free) containing [^{35}S]Met-Cys and nelfinavir and exposed to hypoxia (0.2% oxygen) for 3 hours. Thereafter, cells were lysed and equal amounts of proteins were immunoprecipitated with a HIF-1α antibody. Immunoprecipitated proteins were electrophoresed and vacuum dried and autoradiographed. Equal amounts of proteins were run on SDS-PAGE gel and Western blotting was done for β-actin. HIF level at the bottom of figure refers to ratio of HIF-1α level to β-actin level (as determined by densitometry) normalized to first lane.

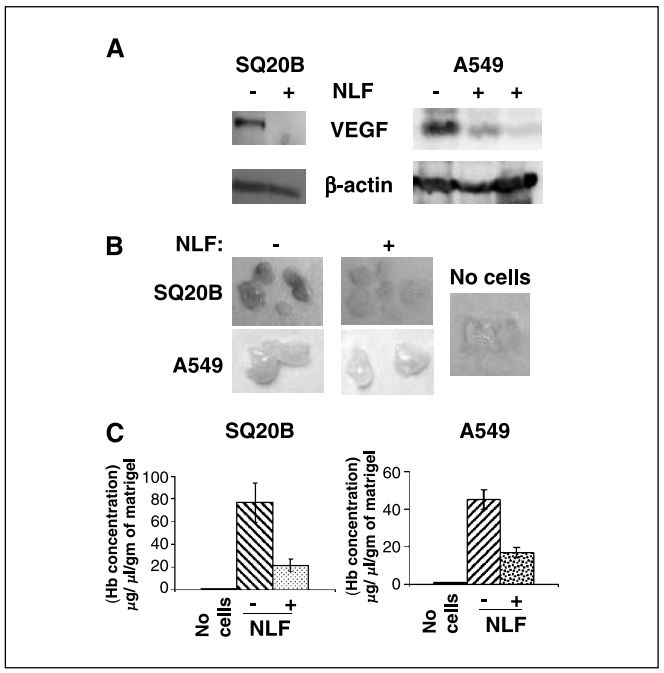

Figure 4. Nelfinavir inhibits *in vivo* angiogenesis and VEGF expression. *A,* mice were injected with SQ20B or A549 cells s.c. on day 1. On day 8, mice were fed diet containing nelfinavir (1.58 mg/d) for 5 days. Thereafter, mice were sacrificed and tumors were harvested for protein; Western blotting was done with VEGF and β-actin antibody (loading control). *B,* Matrigel mixture containing A549 or SQ20B cells was injected s.c. into nude mice at sites lateral to the abdominal midline. As a negative control, Matrigel containing 100 μL of PBS was injected in a similar way. Thereafter, mice were given feed containing nelfinavir, as described earlier. Animals were sacrificed 5 days after injection. The mouse skin was detached along the abdominal midline and the Matrigel plug was recovered and photographed immediately; each discrete mass represents a plug removed from a different animal. *C,* the relative level of hemoglobin present in each plug was determined using commercially available kit. The amount of hemoglobin was calculated from standard hemoglobin curve. *Y axis,* the amount of hemoglobin normalized to the weight of each Matrigel plug.

located in the proximal promoter, and to transactivation of the VEGF promoter (13, 30). Our data show that nelfinavir decreases VEGF expression by down-regulating this pathway (Supplementary Fig. S2). We found that the drug leads to decreased Sp1 phosphorylation (Fig. 2*C*), decreased binding of Sp1 to the proximal core VEGF promoter (Fig. 2*B*), and decreased transactivation of the VEGF promoter (Fig. 2*A*). A separate mechanism by which nelfinavir reduces VEGF expression is by decreasing HIF-1α expression, likely by decreasing protein translation, which leads to decreased induction of VEGF under hypoxia (Fig. 3).

What is the functional consequence of inhibition of HIF-1α and VEGF by nelfinavir? Nelfinavir-treated A549 tumors grown in Matrigel plugs in nude mice showed a reduction in angiogenesis. This therapy did *not* lead to reduced tumor regrowth but did augment the radiation response. A single dose of 8 Gy had minimal effect on tumor regrowth, but in combination with nelfinavir, there was a statistically significant response. We also showed that nelfinavir increases intrinsic radiosensitivity of A549 cells *in vitro*. This is likely to be related to down-regulation of the PI3K/Akt pathway, of which activation has previously shown to be associated with radioresistance (22, 31–34). In addition to this effect, our data suggest that the drug has additional *in vivo* effects on the tumor microenvironment that may contribute to radiosensitization. A recent report suggests that HIF-1 blockade can promote tumor radiosensitization (28). There are a number of reports in the literature that suggest that decreasing VEGF expression following radiation can augment the response of tumors to radiation *in vivo* (26, 27, 29). Therefore, decreasing VEGF and/or HIF-1α expression in these tumors possibly allows for radiosensitization even if nelfinavir by itself does not retard tumor growth.

Our data offer an alternative explanation by which nelfinavir might radiosensitize tumors *in vivo*. Nelfinavir treatment of mice bearing A549 xenografts led to decreased hypoxia in the

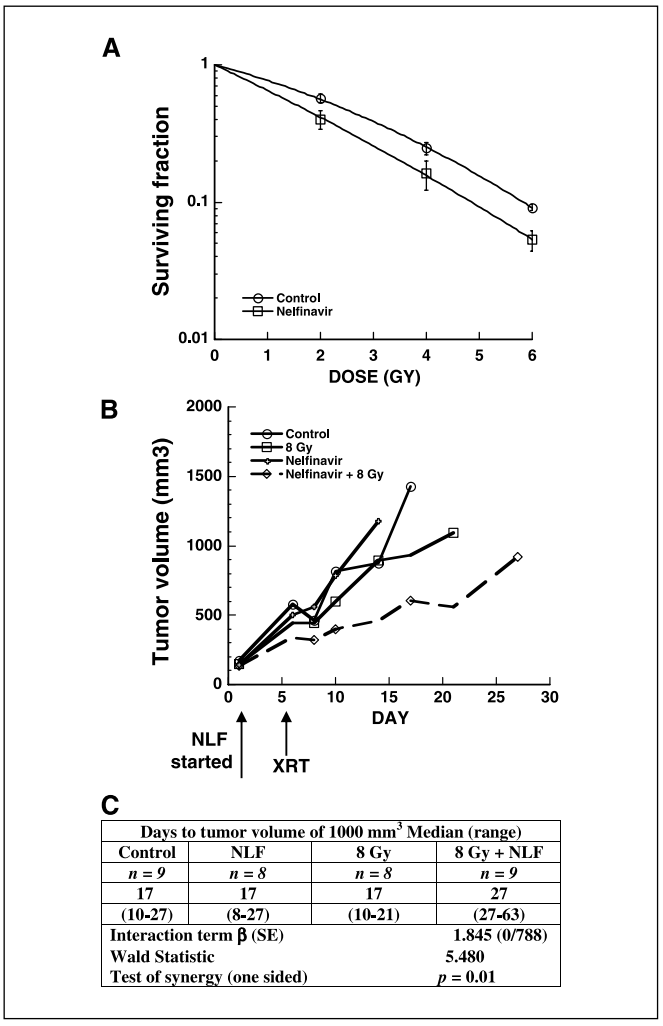

C

Days to tumor volume of 1000 mm^3 Median (range)			
Control	NLF	8 Gy	8 Gy + NLF
n = 9	*n = 8*	*n = 8*	*n = 9*
17	17	17	27
(10-27)	(8-27)	(10-21)	(27-63)
Interaction term β (SE)			1.845 (0/788)
Wald Statistic			5.480
Test of synergy (one sided)			$p = 0.01$

Figure 5. Nelfinavir radiosensitization of A549 cells *in vivo* and *in vitro*. *A, in vitro* clonogenic survival assay for A549 cells treated with nelfinavir (10 μmol/L) or carrier (control) for 1 hour before irradiation. Survival fraction is plotted on *Y* axis versus dose of radiation on *X* axis. *Top curve,* cells treated with control carrier (ethanol); *bottom curve,* nelfinavir-treated cells. The plating efficiency for the cells without nelfinavir (no radiation) was 37% whereas with drug (no radiation) it was 28%. All surviving fractions with radiation were normalized to these baseline plating efficiencies. The drug enhancement factor for a surviving fraction of 0.2 was calculated from this curve to be 4.9 Gy/3.8 Gy or 1.29. *B,* regrowth delay of A549 xenografts ± nelfinavir ± radiation. Seven days after implantation, nelfinavir-treated groups were started on their 5-day diet with feed containing the drug (corresponds to day 1). At this time, the volume ranged from 100 to 125 mm^3. On day 5, a single dose of irradiation was given to both the nelfinavir + radiation and radiation alone groups. Arrows indicate when nelfinavir diet was started and when radiation was given as indicated. *C,* test of synergy for regrowth delay in time to reach tumor volume of 1,000 mm^3. Three mice bearing tumors measuring <1,000 mm^3 at day 63 were censored. Except for these three, all mice developed a tumor volume of 1,000 mm^3 before sacrifice.

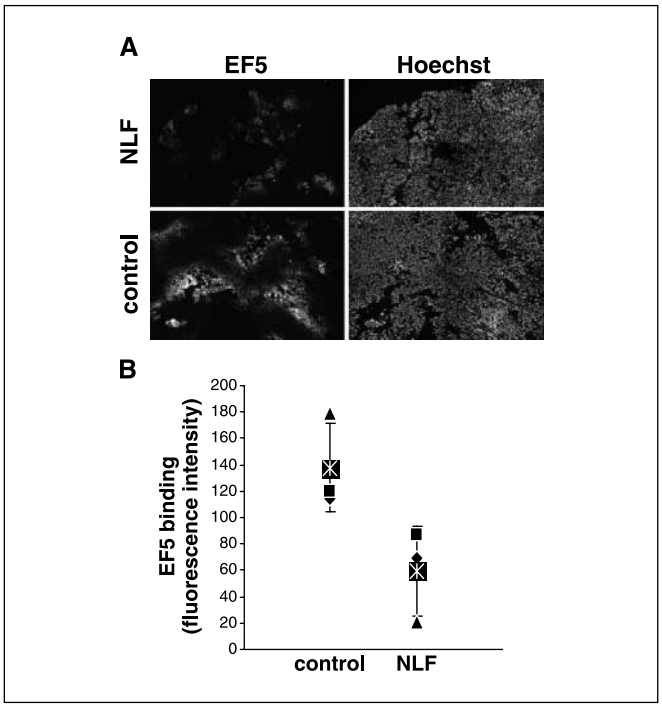

Figure 6. Nelfinavir decreases EF5 binding within A549 xenografts. *A,* mice were injected with A549 cells s.c. on day 1. On day 8, mice were treated with nelfinavir as described before for 5 days. On day 13, mice were injected with EF5, both i.p. and i.v. Three hours later, mice were sacrificed and tumors harvested. Tumors were stained with Hoechst and with the Cy3-conjugated anti-EF5 ELK3-51 antibody. *B,* tumor oxygenation is increased (EF5 binding is decreased) only in tumors treated with nelfinavir. The mean fluorescence intensities of the positively staining regions in individual tumors are shown. *, mean of values obtained in each group; *bars,* SD. Three animals were taken for each group for both control and nelfinavir-treated A549 tumors. Mann-Whitney *U* analysis showed statistical significance for the difference between nelfinavir-treated and control A549 tumors (n = 3 in each group; α_D = 0.05).

tumors. Tumor oxygenation has been of interest to radiobiologists because hypoxic cells are significantly more resistant to cell killing by radiation than are oxic cells. *In vitro* the ratio of the dose required for a given level of cell killing in hypoxia to the dose in air can be 2- to 3-fold higher (35). Under severely hypoxic conditions, there is much less radiation-induced DNA damage, hence less cell killing. Similarly, hypoxia is an important factor in the *in vivo* radiation response. Whereas the pO_2 of normal tissues ranges from 30 to 60 mm Hg, the pO_2 of human cancers is often <5 to 10 mm Hg (36, 37). Hypoxia in human tumors correlates with a poor outcome following radiotherapy in carcinomas of head and neck and uterine cervix (38–41). Thus, enhanced tumor oxygenation of tumors would increase radiation killing. In addition, tumor reoxygenation improves the therapeutic ratio because the radiosensitivity of normal tissues, which are generally not hypoxic, would be expected to be unaltered.

Our data suggest that one mechanism by which nelfinavir radiosensitizes A549 xenografts is by increasing tumor oxygenation. Farnesyltransferase inhibitors also radiosensitize tumors *in vivo* and decrease tumor hypoxia (42). The mechanism of reoxygenation is unknown but may be due to decreased tumor cell oxygen consumption or increased oxygen delivery to the tumor cells. Antiangiogenic agents have also been shown to increase tumor oxygenation *in vivo* (16, 43). It has been suggested that anti-VEGF therapy may decrease interstitial fluid pressure, leading to improved tumor vessels, or that antiangiogenic therapy "normalizes" remaining tumor vessels, leading to vasculature that can more efficiently oxygenate tissues oxygenation (43, 44). In patients with colon cancer, Willett et al. (45) recently showed that the anti-VEGF antibody bevicizumab led to a reduction in interstitial fluid pressure and changes consistent with vascular renormalization. Because nelfinavir decreases VEGF expression, it could be causing similar changes that lead to increased oxygenation.

Nelfinavir has been in clinical use for the treatment of patients with HIV for a decade. It has a good safety profile although it can cause insulin resistance and diabetes (46). Our results suggest that the drug decreases HIF-1α and VEGF expression as well as tumor hypoxia, which could play a role in its *in vivo* radiosensitizing effect. These data support the use of nelfinavir in combination with radiation in future clinical trials.

Acknowledgments

Received 4/7/2006; revised 6/22/2006; accepted 7/12/2006.

Grant support: Public Health Service grants R01 CA093638 (A. Maity), P01CA075138 (S.M. Hahn), R01CA095160 (S.M. Hahn), and R01CA074071 (C.J. Koch), and a Glaxo Smith Kline research grant (A.K. Gupta).

The costs of publication of this article were defrayed in part by the payment of page charges. This article must therefore be hereby marked *advertisement* in accordance with 18 U.S.C. Section 1734 solely to indicate this fact.

We thank J. Wu for excellent technical assistance with the EF5 staining and analysis.

References

1. Gupta AK, Cerniglia GJ, Mick R, McKenna WG, Muschel RJ. HIV protease inhibitors block Akt signaling and radiosensitize tumor cells both *in vitro* and *in vivo*. Cancer Res 2005;65:8256–65.
2. Altomare DA, Testa JR. Perturbations of the AKT signaling pathway in human cancer. Oncogene 2005;24:7455–64.
3. Hennessy BT, Smith DL, Ram PT, Lu Y, Mills GB. Exploiting the PI3K/AKT pathway for cancer drug discovery. Nat Rev Drug Discov 2005;4:988–1004.
4. Vivanco I, Sawyers CL. The phosphatidylinositol 3-Kinase AKT pathway in human cancer. Nat Rev Cancer 2002;2:489–501.
5. Cantley LC, Neel BG. New insights into tumor suppression: PTEN suppresses tumor formation by restraining the phosphoinositide 3-kinase/AKT pathway. Proc Natl Acad Sci U S A 1999;96:4240–5.
6. Haas-Kogan D, Shalev N, Wong M, Mills G, Yount G, Stokoe D. Protein kinase B (PKB/Akt) activity is elevated in glioblastoma cells due to mutation of the tumor suppressor PTEN/MMAC. Curr Biol 1998;8:1195–8.
7. Yamada KM, Araki M. Tumor suppressor PTEN: modulator of cell signaling, growth, migration and apoptosis. J Cell Sci 2001;114:2375–82.
8. Zhong H, Chiles K, Feldser D, et al. Modulation of hypoxia-inducible factor 1α expression by the epidermal growth factor/phosphatidylinositol 3-kinase/PTEN/AKT/FRAP pathway in human prostate cancer cells: implications for tumor angiogenesis and therapeutics. Cancer Res 2000;60:1541–5.
9. Zundel W, Schindler C, Haas-Kogan D, et al. Loss of PTEN facilitates HIF-1-mediated gene expression. Genes Dev 2000;14:391–6.
10. Maxwell PH. Hypoxia-inducible factor as a physiological regulator. Exp Physiol 2005;90:791–7.
11. Carmeliet P. VEGF as a key mediator of angiogenesis in cancer. Oncology 2005;69 Suppl 3:4–10.
12. Ferrara N. VEGF as a therapeutic target in cancer. Oncology 2005;69 Suppl 3:11–6.
13. Pore N, Liu S, Shu HK, et al. Sp1 is involved in Akt-mediated induction of VEGF expression through an HIF-1-independent mechanism. Mol Biol Cell 2004;15:4841–53.
14. Dignam JD, Lebovitz RM, Roeder RG. Accurate transcription initiation by RNA polymerase II in a soluble extract from isolated mammalian nuclei. Nucleic Acids Res 1983;11:1475–89.
15. Koch CJ, Evans SM, Lord EM. Oxygen dependence of cellular uptake of EF5 [2-(2-nitro-1*H*-imidazol-1-yl)-*N*-(2,2,3,3,3-pentafluoropropyl)acetamide]: analysis of drug adducts by fluorescent antibodies vs bound radioactivity. Br J Cancer 1995;72:869–74.
16. Lee J, Siemann DW, Koch CJ, Lord EM. Direct relationship between radiobiological hypoxia in tumors

and monoclonal antibody detection of EF5 cellular adducts. Int J Cancer 1996;67:372–8.
17. Evans SM, Joiner B, Jenkins WT, Laughlin KM, Lord EM, Koch CJ. Identification of hypoxia in cells and tissues of epigastric 9L rat glioma using EF5 [2-(2-nitro-1*H*-imidazol-1-yl)-*N*-(2,2,3,3,3-pentafluoropropyl) acetamide]. Br J Cancer 1995;72:875–82.
18. Busch TM, Wileyto EP, Emanuele MJ, et al. Photodynamic therapy creates fluence rate-dependent gradients in the intratumoral spatial distribution of oxygen. Cancer Res 2002;62:7273–9.
19. Evans SM, Jenkins WT, Joiner B, Lord EM, Koch CJ. 2-Nitroimidazole (EF5) binding predicts radiation resistance in individual 9L s.c. tumors. Cancer Res 1996;56: 405–11.
20. Koch CJ. Measurement of absolute oxygen levels in cells and tissues using oxygen sensors and the 2-nitroimidazole EF5. In: Sen C, Packer L, editors. Methods in enzymology: antioxidants and redox cycling. San Diego: Academic Press; 2002. p. 3–31.
21. Juarez JC, Guan X, Shipulina NV, et al. Histidine-proline-rich glycoprotein has potent antiangiogenic activity mediated through the histidine-proline-rich domain. Cancer Res 2002;62:5344–50.
22. Gupta AK, Cerniglia GJ, Mick R, et al. Radiation sensitization of human cancer cells *in vivo* by inhibiting the activity of PI3K using LY294002. Int J Radiat Oncol Biol Phys 2003;56:846–53.
23. Rohlff C, Ahmad S, Borellini F, Lei J, Glazer RI. Modulation of transcription factor Sp1 by cAMP-dependent protein kinase. J Biol Chem 1997;272: 21137–41.
24. Pal S, Datta K, Khosravi-Far R, Mukhopadhyay D. Role of protein kinase Czeta in Ras-mediated transcriptional activation of vascular permeability factor/vascular endothelial growth factor expression. J Biol Chem 2001;276:2395–403.
25. Fojas de Borja P, Collins NK, Du P, Azizkhan-Clifford J, Mudryj M. Cyclin A-CDK phosphorylates Sp1 and enhances Sp1-mediated transcription. EMBO J 2001;20: 5737–47.
26. Gorski DH, Beckett MA, Jaskowiak NT, et al. Blockage of the vascular endothelial growth factor stress response increases the antitumor effects of ionizing radiation. Cancer Res 1999;59:3374–8.
27. Hess C, Vuong V, Hegyi I, et al. Effect of VEGF receptor inhibitor PTK787/ZK222584 [correction of ZK222548] combined with ionizing radiation on endothelial cells and tumour growth. Br J Cancer 2001;85:2010–6.
28. Moeller BJ, Dreher MR, Rabbani ZN, et al. Pleiotropic effects of HIF-1 blockade on tumor radiosensitivity. Cancer Cell 2005;8:99–110.
29. Zips D, Eicheler W, Geyer P, et al. Enhanced susceptibility of irradiated tumor vessels to vascular endothelial growth factor receptor tyrosine kinase inhibition. Cancer Res 2005;65:5374–9.
30. Pore N, Jiang Z, Gupta A, Cerniglia G, Kao G, Maity A. EGFR tyrosine kinase inhibitors decrease vascular endothelial growth factor (VEGF) expression by both hypoixa inducible factor (HIF)-1 indepdent and dependent mechanisms. Cancer Res 2006;66:197–204.
31. Grana TM, Rusyn EV, Zhou H, Sartor CI, Cox AD. Ras mediates radioresistance through both phosphatidylinositol 3-kinase-dependent and Raf-dependent but mitogen-activated protein kinase/extracellular signal-regulated kinase kinase-independent signaling pathways. Cancer Res 2002;62:4142–50.
32. Gupta AK, Bakanauskas VJ, Cerniglia GJ, et al. The Ras radiation resistance pathway. Cancer Res 2001;61: 4278–82.
33. Nakamura JL, Karlsson A, Arvold ND, et al. PKB/Akt mediates radiosensitization by the signaling inhibitor LY294002 in human malignant gliomas. J Neurooncol 2005;71:215–22.
34. Kim IA, Bae SS, Fernandes A, et al. Selective inhibition of Ras, phosphoinositide 3 kinase, and Akt isoforms increases the radiosensitivity of human carcinoma cell lines. Cancer Res 2005;65:7902–10.
35. Koch CJ, Kruuv J, Frey HE. Variation in radiation response of mammalian cells as a function of oxygen tension. Radiat Res 1973;53:33–42.
36. Brown JM, Wilson WR. Exploiting tumour hypoxia in cancer treatment. Nat Rev Cancer 2004;4:437–47.
37. Evans SM, Koch CJ. Prognostic significance of tumor oxygenation in humans. Cancer Lett 2003;195:1–16.
38. Brizel DM, Sibley GS, Prosnitz LR, Scher RL, Dewhirst MW. Tumor hypoxia adversely affects the prognosis of carcinoma of the head and neck. Int J Radiat Oncol Biol Phys 1997;38:285–9.
39. Fyles AW, Milosevic M, Wong R, et al. Oxygenation predicts radiation response and survival in patients with cervix cancer. Radiother Oncol 1998;48:149–56.
40. Gatenby RA, Kessler HB, Rosenblum JS, et al. Oxygen distribution in squamous cell carcinoma metastases and its relationship to outcome of radiation therapy. Int J Radiat Oncol Biol Phys 1988;14:831–8.
41. Hockel M, Schlenger K, Aral B, Mitze M, Schaffer U, Vaupel P. Association between tumor hypoxia and malignant progression in advanced cancer of the uterine cervix. Cancer Res 1996;56:4509–15.
42. Cohen-Jonathan E, Evans SM, Koch CJ, et al. The farnesyltransferase inhibitor L744,832 reduces hypoxia in tumors expressing activated H-ras. Cancer Res 2001; 61:2289–93.
43. Winkler F, Kozin SV, Tong RT, et al. Kinetics of vascular normalization by VEGFR2 blockade governs brain tumor response to radiation: role of oxygenation, angiopoietin-1, and matrix metalloproteinases. Cancer Cell 2004;6:553–63.
44. Jain RK. Normalization of tumor vasculature: an emerging concept in antiangiogenic therapy. Science 2005;307:58–62.
45. Willett CG, Boucher Y, di Tomaso E, et al. Direct evidence that the VEGF-specific antibody bevacizumab has antivascular effects in human rectal cancer. Nat Med 2004;10:145–7.
46. Powderly WG. Long-term exposure to lifelong therapies. J Acquir Immune Defic Syndr 2002;29 Suppl 1:S28–40.